

SIM-DSP: A DSP-Enhanced CAD Platform for Signal Integrity Macromodeling and Simulation

Chi-Un LEI

Department of Electrical and Electronic Engineering, The University of Hong Kong, Hong Kong

culei@eee.hku.hk

Abstract. *Macromodeling-Simulation process for signal integrity verifications has become necessary for the high speed circuit system design. This paper aims to introduce a “VLSI Signal Integrity Macromodeling and Simulation via Digital Signal Processing Techniques” framework (known as SIM-DSP framework), which applies digital signal processing techniques to facilitate the SI verification process in the pre-layout design phase. Core identification modules and peripheral (pre-/post-)processing modules have been developed and assembled to form a verification flow. In particular, a single-step discrete cosine transform truncation (DCTT) module has been developed for modeling-simulation process. In DCTT, the response modeling problem is classified as a signal compression problem, wherein the system response can be represented by a truncated set of non-pole-based DCT bases, and error can be analyzed through Parseval’s theorem. Practical examples are given to show the applicability of our proposed framework.*

Keywords

Simulation, signal integrity, high-speed circuits, macromodeling.

1. Introduction

Radio-frequency systems and electronic systems, such as mobile communication systems and high-speed computers, have become essential to our daily lives. These electronic systems contain modules of integrated circuits (ICs). These modules are connected by signal and power distribution networks [1], [2]. With the increasing operation frequency and decreasing feature size of ICs, high-frequency effects of the network, such as signal delay, reflections, crosstalk and simultaneous switching noise, have significantly disturbed the original signals, and have become dominant factors that limit IC system performance [3], [4]. Therefore, signal integrity (SI) verification has become popular practices in the IC design process to address such limitations, so as to ensure consistent signal transmissions and reliable power distributions in high-speed electronic systems [5]. In the pre tape-out phase, detailed simulation and analysis

are required to capture the high-frequency behaviors of systems. However, a full-wave electromagnetic (EM) analysis over the global system is impractical. Reduced (simplified) models, which preserve relevant properties from the original models, are therefore required for time-critical simulations. In particular, for structures with complicated geometry, such as packages, vias and radio-frequency (RF) objects, data-driven macromodeling is usually applied to generate reduced models. Responses of systems are usually approximated using s -domain Sanathanan-Koerner (SK) iteration [6] or equivalent discrete-time domain (z -domain) Steiglitz-McBride (SM) iteration [7].

Different stand-alone macromodeling algorithms [8]-[9] have been developed. However, peripheral processing techniques have not been developed. Therefore, they are not capable for a functional modeling-simulation-analysis process. Besides them, there are some comprehensive modeling-simulation methodologies. MATLAB RF toolbox [10] and IdEM toolbox [11] have adopted Vector Fitting (VF) [8] as the core identification algorithm for the modeling-simulation process. However, they suffer from ill-conditioned problems because of the iterative computation property. IBM AQUAIA [12], [13] provides a comprehensive simulation for on-chip interconnect analysis with an in-built EM field solver. However, it does not apply model order reduction techniques; therefore, often generate large scale models, which are not efficient for practical simulations. Another methodology BEMP [14], [15] constructs macromodels using a cascade of low-/band-/high-/all-pass filters, however it has a large computation complexity, which also makes it not practical for simulations. Meanwhile, discrete-time domain computations of transient simulation have been introduced to exploit its nice features [16].

Furthermore, besides improving the macromodeling process from a mathematical (mostly control-theoretic) perspective, pre-/post-processing techniques and improvement from non-control-theoretic perspectives have been less explored in the literature. Also, due to the emerging development of microelectronics features [3], [17], new considerations and new necessities have been raised for developments of the SI verification process. Existing standard macromodeling approaches have a room for improvement in modeling new interconnect features. Therefore, advanced macromod-

eling methodologies should be developed to meet the needs of SI simulations [18].

In this paper, a “VLSI Signal Integrity Macromodeling and Simulation via Digital Signal Processing Techniques” (SIM-DSP) framework is proposed for an effective interconnect macromodeling and simulation process [19]. This framework explores the feasibility and benefits of applying digital signal processing (DSP) techniques in the macromodeling process. We first give an introduction of SI (Section 2). Then we outline the macromodeling-simulation methodology flow and developed modules in the framework (Section 3). Various case studies are given to show the applicability and effectiveness of our proposed framework and algorithm (Section 4).

There are several contributions in this paper. First, a discrete cosine transform truncation (DCTT) approach is presented for the modeling-simulation process of time- and frequency-sampled responses. The response modeling is classified as a signal compression problem, such that DCTT provides a numerical-insensitive and simple computation with an exact *a priori* error analysis through Parseval’s theorem. Second, the developed identification modules and peripheral processing modules have been assembled to form a functional modeling-simulation flow for SI verifications. Third, several benchmarks of industrial interest have been performed and are documented in this paper, with explanations of influences of macromodeling-simulation process in SI verifications.

2. Signal Integrity and Macromodeling

SI generally refers to problems that occur in the high speed circuit system due to physical interconnects. It happens as an EM phenomenon in nature. However, as ICs move toward the era of nano-scale and multi-GHz-operation, SI problems now become the bottleneck of the high speed system design. SI issues disturb the signal voltage, and make the transmitted signal become ambiguous. As a result, the quality of the signal transmission and the circuit performance are degraded by the disturbance, especially in high speed circuits. Discussions about SI can be found in [20], [21].

To reduce the design risk and shorten the design period of sophisticated circuits, modeling, simulation and verification process is developed, such that the electrical performance of the emerging inter-/intra-chip communication links in circuit systems can be simulated for *a priori* diagnosis.

To model a complicated geometry structure, generally, for a single-port system, macromodeling techniques intend to fit a linear time-invariant (LTI) system to the desired continuous-time frequency domain (s -domain) input/output (I/O) response $H(s)$ at a set of calculated/sampled points at the I/O ports. The model is usually a state-space system

or a rational transfer function with a set of predefined basis $\{\phi_n\}$

$$H(s) \approx \frac{N(s)}{D(s)} = \frac{\sum_{n=1}^N b_n \phi_n(s)}{\sum_{n=1}^N \tilde{b}_n \phi_n(s)} \quad (1)$$

where $\tilde{b}_n, b_n \in \mathbb{R}$ and N is the macromodel order. Therefore, macromodeling can be regarded as a large-scale broadband system identification problem.

In the L_2 -norm sense with N_s sampled points, the optimal model of a system can be obtained through minimizing the following objective function

$$\min \sum_{k=1}^{N_s} \left\| \frac{N(s_k)}{D(s_k)} - H(s_k) \right\|_2. \quad (2)$$

However, this is a numerically sensitive non-linear problem with no prior information about the exact pole and zero locations of the system.

3. SIM-DSP Methodology Flow

SIM-DSP framework aims to explore the feasibility and benefits of applying DSP techniques in the macromodeling process, in order to improve the functionality and accuracy of the macromodeling-simulation process in a comprehensive manner, from the initial response characterization step to the final simulation step. The focus of this framework is on

1. Improving the functionality and automation of the identification process;
2. Increasing the fitting accuracy of the identification process;
3. Reducing the computation time of the macromodeling procedure.

A generic SIM-DSP macromodeling-simulation methodology flow in SIM-DSP is shown in Fig. 1., while Fig. 2 shows the data and process flow chat in SIM-DSP. The sampled structure responses can be obtained by exciting one input port at a time and then directly measuring the responses at the output ports by instruments [21] or computing the responses by the given structure geometries and the EM field solver [22] (**Response Characterization**). Sampled data are analyzed for *a priori* configuration in the later identification process, such as selecting the macromodel order and number of iteration. At the same time, sampled data are processed for the enhancement of identifications (**Data Pre-processing**). By approximating the processed system response data in a black-box approach with the determined configuration, a macromodel is generated to replace the original large-order system by a smaller-order one with similar input-output (I/O) behaviors (**Macromodeling**), in form of a rational function

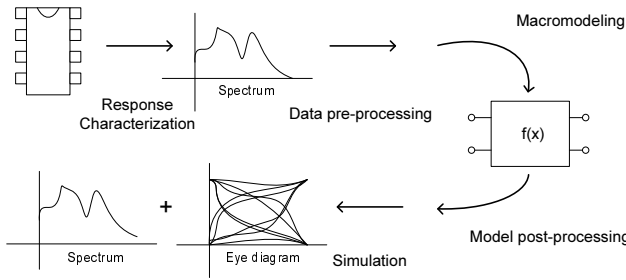


Fig. 1. Macromodeling-Simulation flow in SIM-DSP in a generic perspective.

model, a pole-residue model, or a combination of specific bases. Then post-processing techniques are used to modify the macromodel characteristics and enhance the simulation performance (**Model Post-processing**), based on the macromodel and the peripheral information in the identification process. At last, the processed macromodel is used to produce spectra and waveforms numerically for SI analysis (e.g. eye diagram analysis and Bit Error Rate (BER) analysis), and/or converted into a circuit level model (e.g. SPICE equivalent circuit) or a mathematical model and coupled with other circuit model blocks for a global simulation (**Simulation**). In summary, SIM-DSP exploits nice features of discrete-time domain computations [16].

Currently, SIM-DSP framework has built up the following functional modules:

- Data pre-processing module for macromodeling configurations;
- System identification module for frequency-domain macromodeling;
- System identification module for time-domain macromodeling;
- Simulation module for real-time SI verifications;
- Modeling-Simulation module for time-domain SI verifications.

All these are captured and presented in the following subsections. Follow-up discussions are also shown in Section 3.6.

3.1 Data Pre-processing: Macromodeling Process Enhancement via Frequency Warping

To alleviate ill-conditioned computation problems in the linear-structure macromodeling process, we have proposed a spectral pre-processing scheme frequency warping. Frequency warping transforms the structure response, in order to introduce a numerically favorable fitting in the frequency domain, and to improve the fitting accuracy during

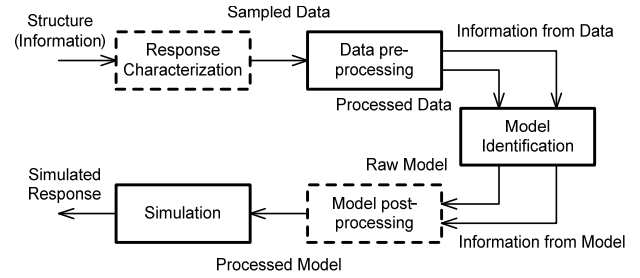


Fig. 2. Macromodeling-Simulation flow in SIM-DSP in a data-process perspective.

the macromodeling process. The structure response is transformed by frequency warping which assigns an effective weighting in the frequency domain and gives a higher resolution (accuracy) in the desired region during computation.

3.2 Macromodeling: Macromodeling Framework Advancements via Discrete Time Domain Computation

To enhance the numerical robustness and functionality of the widely adopted, iterative based VF framework, we have proposed a family of improvements based on the root of the z -domain computation [23]. In the first part, we have shown some features and advantages of z -domain computation in the macromodeling process. Then, we have proposed the z -domain counterpart of VF (VFz), which uses z -domain partial fraction basis to seek a rational approximation to the desired response, namely,

$$\hat{f}(z) = \left(\sum_{b=1}^B \frac{c_b}{1 - z^{-1}a_b} \right) + d \approx f(z) \quad (3)$$

where B is the number of basis. This improves the numerical conditioning and convergence in broadband frequency-sampled system macromodeling.

In the second part, we have extended VFz as a functionality-oriented macromodeling algorithm. First, we have extended VFz to its time-domain (TD-VFz) [24] variants for the specific time domain macromodeling purpose. TD-VFz does not require discretizing the continuous-time convolution integrals for each iteration and it provides *a priori* model order selection through Hankel Singular Values (HSVs) computation as a pre-processing process. Second, we have also proposed the hybrid-domain (HD-VFz) variants, which model responses with a better hybrid-domain accuracy through providing extra informative data. Third, we have developed a versatile macromodeling adoption through a P -norm approximation expansion. We have modeled various structures, from chip-level to board-level, via VFz to demonstrate its excellent performance.

3.3 Macromodeling: Multiport Macromodeling Technique without Eigenvalue Computation and Initial Guess

To avoid numerically sensitive initial guess and expensive computation in time-domain macromodeling process, we have developed rational function macromodeling algorithms (VISA [25] and WISE [26]) for accuracy-oriented macromodeling. The idea is to regard the system response as the impulse response of a finite-impulse-response (FIR) filter, and then apply infinite-impulse-response (IIR) filter approximation techniques to generate the macromodel. By applying the idea of Walsh theorem and complementary signal, this approach can be interpreted as an interpolation problem. This approach can be interpreted as a numerically simple, non-pole-based Steiglitz-McBride (SM) iteration without initial guess and eigenvalue computation.

3.4 Simulation: Real-time Simulation for Emerging Interconnect System SI Verifications

Computed macromodels are used to generate responses for later-stage simulations and verifications. A visual simulation platform is realized using Matlab Simulink, for multi-level SI simulations and analysis, because of the following reasons,

1. Simulations can be easily coupled with other physical-domain blocks and simulation platforms through a simple interface, in order to model mechanical, thermal and other physical characteristics of nano-scale circuits and give a more realistic transient simulation.
2. Complex models can be segmented into hierarchies of design components (blocks), with levels of abstractions. Thus, this helps the division of labor and shortens the design cycle.
3. Tested signal in the simulation process can be generated and monitored in a real-time manner. The simulation process becomes convenient to examine simulation results, analysis the performance and diagnose unexpected and inconsistent behaviors in the simulation. Thus, the design cycle can be shortened.
4. Signal properties, such as clock jitter, signal delay and signal noise, can be modeled with supplemental components and a quick configuration, for a more realistic simulation.

3.5 Modeling-Simulation: Single-Step Modeling-Simulation via Discrete Cosine Transform Truncation (DCTT)

Different macromodeling techniques have been proposed. However, most of them are based on iterative methods with fundamental drawbacks. On the other hand, im-

pulse response models have been introduced for SI simulation with the help of efficient convolution methods [27], [28]. However, impulse response models contain lots of parameters, which are not effective for model storing and response computation. Therefore, a compacted model formulation is proposed in this section.

Discrete Cosine Transform (DCT), which is a generalization of the Discrete Fourier Transform (DFT), has been proposed to represent the (discrete) time-sampled sequences using a set of energy-compacted, orthogonal, real-valued basis sequences [29]. In general, DCT is superior to all other discrete transforms in terms of accuracy [29]. In the mean time, DCT inherits some properties in DFT, such as basis orthogonality and unity, while the symmetrical extension property in DCT reduces the abruptness of truncation, when compared to the DFT. Therefore, it has been used in audio/visual signal compression and coding [29], as well as combinational circuit current simulation [30].

In this section, a discrete cosine transform truncation (DCTT) method is proposed for time- and frequency-sampled modeling-simulation in the discrete-time domain, in which the system response is modeled by a small number of DCT bases instead of a rational model. Two main features of DCTT are:

1. DCTT handles the macromodeling problem as a single-step signal compression problem instead of a numerical-sensitive system identification problem, which avoids many drawbacks in the iterative approach.
2. DCTT provides an exact *a priori* error analysis through Parseval's theorem for model size selection.

3.5.1 Decomposition and Reconstruction of Sampled Responses using DCT

Assuming a N -point (discrete) time-sampled output signal sequence is given ($x[n]$ for $n = 0, 1, \dots, N-1$), and the input signal sequence is a normalized impulse response ($i[0] = 1$ and $i[n] = 0$ for $n = 1, \dots, N-1$), we would approximate the finite-length time-sampled signal sequences using a truncated set of orthogonal spectral bases $\phi_k[n]$

$$x[n] = \sum_{k=0}^{N-1} X[k] \phi_k[n]. \quad (4)$$

Having assumptions of both periodicity ($x[n] = x[nT]$ for $n = 0, 1, \dots, N-1$, where T is the sampling period) and even symmetry (i.e., a symmetrically extended sequence x_2 exists, where $x_2[n] = x[n]$ for $n = 0, 1, \dots, N-1$ and $x_2[n] = x[2N-1-n]$ for $n = N, N+1, \dots, 2N-1$), DCT-II (the most commonly used DCT) uses periodic cosine function as basis. DCT decomposes the sampled response signal into a summation of DCT bases

$$X_{DCT}[k] = \sqrt{\frac{2}{N}} \beta[k] \sum_{n=0}^{N-1} x[n] \cos\left(\frac{\pi k(2n+1)}{2N}\right), \quad (5)$$

for $k = 0, 1, \dots, N-1$, where β is a normalization factor, and $\beta[k] = \frac{1}{\sqrt{2}}$ for $k = 0$ and 1 for $k = 1, 2, \dots, N-1$. The response can be reconstructed using the inverse discrete cosine transform (IDCT)

$$x[n] = \sqrt{\frac{2}{N}} \beta[k] \sum_{k=0}^{N-1} X_{DCT}[k] \cos\left(\frac{\pi k(2n+1)}{2N}\right), \quad (6)$$

for $n = 0, 1, \dots, N-1$.

Meanwhile, an N -point DCT X_{DCT} is closely related to a $2N$ -point DFT X_{DFT} of the N -point signal sequence $x[n]$,

$$X_{DCT}[k] = 2\Re\left\{X_{DFT}[k] e^{-j\pi k/(2N)}\right\}, \quad (7)$$

for $k = 0, 1, \dots, N-1$. The relation from $X_{DCT}[k]$ to $X_{DFT}[k]$ is not as straightforward as from $X_{DFT}[k]$ to $X_{DCT}[k]$, but a relationship can be derived,

$$X_{2-DFT}[k] = \begin{cases} X_{DCT}[0] & k=0, \\ e^{j\pi k/2N} X_{DCT}[k] & k=1, \dots, N-1, \\ 0 & k=N, \\ -e^{j\pi k/2N} X_{DCT}[2N-k] & k=N+1, \dots, 2N-1 \end{cases} \quad (8)$$

where $X_{2-DFT}[k]$ is the $2N$ -point DFT of the $2N$ -point symmetrically extended sequence $x_2[n]$ of the response sequence $x[n]$. If inverse DFT is applied to X_{2-DFT} , we obtain

$$x_2[n] = \frac{1}{2N} \sum_{k=0}^{2N-1} X_{2-DFT}[k] e^{j2\pi kn/(2N)} \quad (9)$$

and $x[n] = x_2[n]$ for $n = 0, 1, \dots, N-1$, then we can apply DFT to obtain X_{DFT} (frequency-sampled response).

3.5.2 Response Decomposition and Basis Truncation in DCTT

As discussed in the previous section, we can obtain DCT coefficients from arbitrary frequency-sampled data (DFT coefficients) or arbitrary time-sampled impulse response through (7) or (5), respectively. Similar to DFT, according to the Parseval's theorem, the total energy contained in the time-sampled signal is equal to the total energy of the DCT bases. Therefore, the signal energy can be separated into the energy of an approximant signal E_{DCT} and the energy of an error signal E_{error} , namely,

$$\begin{aligned} \sum_{n=0}^{N-1} |x(n)|^2 &= \frac{1}{N} \sum_{n=0}^{N-1} \beta(k) |X_{DCT}(k)|^2 \\ &= \underbrace{\frac{1}{N} \sum_{n=0}^{N_{pr}-1} \beta(k) |X_{DCT}(k)|^2}_{E_{DCT}} + \underbrace{\frac{1}{N} \sum_{n=N_{pr}}^{N-1} \beta(k) |X_{DCT}(k)|^2}_{E_{error}} \end{aligned} \quad (10)$$

where N_{pr} is the number of the preserved DCT bases. Therefore, the exact error E_{error} can be calculated from the truncated bases, which allows *a priori* error analysis and a per-

ceptual model size selection to facilitate the macromodeling process. Furthermore, as DCTT uses real-coefficient bases, the algorithm generates real-valued output signal for real-valued input signal with truncation of arbitrary number of bases. Also, DCTT avoids extra considerations (and computations) in rational-function fitting approaches to handle response with complex conjugate poles as DCTT does not model the response using its pole information.

In general, DCTT reduces the system order significantly for lowpass-response signals, which is common for many physical systems. It is also shown that DCT is nearly optimum in the sense of minimum mean-squared truncation error for sequences with exponential correlation functions [29], which makes DCTT superior in modeling exponentially decaying physical system responses.

3.5.3 Response Reconstruction in DCTT

As discussed in the previous section, the response signal can be perfectly reconstructed by (6). By truncating insignificant bases, i.e., $X_{DCT}[k] := 0$ for k with small $|X_{DCT}[k]|^2$, the time-sampled signal can be almost fully reconstructed, whereas insignificant bases are not calculated and stored. Since all computations in DCTT involve only multiplications (no root-finding nor eigenvalue calculation), it is easy to apply in the high-level simulation environment (e.g., Verilog-A and Matlab). The continuous-time system response can be obtained from the discrete-time system response through a stability- and passivity-preserving bilinear transform ($z = e^{sT} \approx (1 + sT/2)/(1 - sT/2)$).

For electrically long structures (e.g., broad-level transmission line), time delay may exist and cause difficulties in modeling and simulation. In DCTT, to model responses with time delay, the peripheral time delay can be included artificially during the simulation process, or adopted into the DCT basis parameters. The adoption with a unit time delay is described by

$$X_{shift}[m] = \cos\left(\frac{m\pi}{N}\right) X_{DCT}[m] + \sin\left(\frac{m\pi}{N}\right) X_{DST}[m] + \frac{2}{N} \beta[k] [(-1)^m x[n] - x(0)] \cos\left(\frac{m\pi}{2N}\right) \quad (11)$$

where $X_{DST}[m]$ is the Discrete Sine Transform (DST) of the signal $x(n)$, which can be calculated and adopted into DCT parameters during the decomposition stage. An arbitrary time shift can be similarly adopted through the recursion of (11).

3.5.4 Computation Complexity

Similar to DFT, by exploiting the Fast Fourier Transform (FFT) approach, the relationship between DCT and DFT, factorization and the real-valued coefficient property, the computation can be reduced to $N \log N - 3N/2$ real multiplications for a complete DCT. Different implementations have been proposed for different tradeoff [29]. The computation is further reduced in IDCT as most of the DCT bases in the reduced macromodel have been truncated to zero.

Comparing to conventional approaches, DCTT is a non-iterative approach, which is numerically simple (i.e., accurate and efficient) in computation. On the other hand, the computation complexity of the iterative macromodeling approach (e.g. VF(z) and WISE) is $O(kM^2N)$, where M is the model order size, and k is the number of the iterations, which is the computation bottleneck in the iterative approach. Furthermore, DCTT avoids expensive root or eigenvalue calculation, overhead computation (e.g. pole stabilization) and manual effort for selection of model order and number of iterations.

3.5.5 Remarks in Using DCT Basis

Some remarks are in order:

1. Karhunen-Loeve transform (KLT) is shown to be an ideal transform [31], where the most signal energy is contained in the fewest number of bases. However, KLT involves expensive computations to determine the basis. Therefore, discrete cosine transform (DCT) has been proposed. DCT is shown to be the best approximation to KLT among different kinds of transforms in most situations [29].
2. By considering the transform as a generalized Wiener filtering problem, DCT is shown to be less disturbed by additive noise, comparing to other transforms [29]. The uncorrelated white noise signal only affects small-magnitude DCT bases, which will be truncated during macromodeling. The numerically robust performance of DCTT is shown in the numerical examples.
3. To achieve a more accurate modeling of highpass or arbitrary response, warped DCT (WDCT) can be applied for response compensation [32], which bilinearly maps the response to a weighted response for numerically favorable computations. This further enhances the universal performance of DCTT.

3.6 Remarks in SIM-DSP

Some remarks are in order:

1. The purpose of introducing VISA is for accuracy-oriented macromodeling. Its compact formation and specialized time domain properties adoption makes VISA a numerically simple (and thus efficient and accurate) time-domain macromodeling algorithm. These specialties also make VISA difficult for generalizations, such as developing its frequency domain variants. On the other hand, VFz are purposed for the functionality-oriented macromodeling development. As a result, VFz and its variants provide different generalizations for various applications. Meanwhile, DCTT is also introduced for a non-iterative, numerical robust modeling-simulation of arbitrary port-to-port responses. DCTT requires only a single-step computation without knowing the location of poles,

which is much less numerical sensitive to iterative-based computation. However, DCTT is needed to introduce a more direct and convenient interface for ease of simulations.

2. Developed modules may not generate a passivity-guaranteed macromodel. However, passivity check/enforcement techniques in continuous-time domain (as shown in [33]) can be used to rectify the model, since the bilinear continuous-to/from-discrete transformation is passivity-preserving [34]. Furthermore, discussions about passivity in z-domain system can be found in [34].
3. The purpose of applying digital signal processing (DSP) is to represent, transform and manipulate digitized (discretized) signals and information in an organized and meaningful manner [35]. In SIM-DSP, we have leveraged on features of (pre-)processing (Section 3.1), computation in a transformed domain (from Section 3.2 to Section 3.5), sampling (Section 3.1) and architectures (Section 3.3 and 3.5) in the DSP area to benefit VLSI macromodeling and simulation process in a well-rounded perspective.

4. Case Studies Using SIM-DSP Framework

To illustrate the performance of SIM-DSP framework, we model responses of several practical testbenches using SIM-DSP. The proposed framework is coded in Matlab m-script (text) files and runs in the Matlab 7.4 environment on a 1GB-RAM 3.4GHz PC. Table 1 summarizes the implementation analysis of all the examples. A detailed macromodeling-simulation process is shown in the first example. Other examples show the performance of the core macromodeling module using VFz and DCTT.

4.1 A Detailed Macromodeling-Simulation Process of a Four-port Backplane using VFz

A 520 mm differential transmission channel (including Tyco line cards) on a full mesh ATCA Kaparel backplane is designed using the Tyco Quadroute technique [36]. The standard 4-port scattering parameters (4-port) are measured using a vector network analyzer (VNA) over 1497 frequencies ranging from 50 MHz to 15 GHz. The frequency-sampled response of some typical time-delayed port responses are extracted. Each response is fitted using VFz with a 130-pole approximant. Each response takes about 10 iterations and 12 seconds for VFz to reach convergence. Fig. 3 plots the fitted responses. VFz gives an accurate identification result. The implementation analysis is summarized in Tab. 1.

This example shows the numerical difficulties of approximating time-delayed responses using ordinary system

	No. of points per response	No. of responses	Frequency range (Hz)	Types of sampled response	No. of poles	Average relative error	CPU time (sec.)
4-port (1,1)	1497	1	50 M - 15 G	Scattering with delay	130	0.1123	10
4-port (2,1)	1497	1	50 M - 15 G	Scattering with delay	130	0.0928	10
4-port (4,1)	1497	1	50 M - 15 G	Scattering with delay	130	0.0755	10
IEEE.802 (3,1)	1496	1	50 M - 15 G	Scattering	136	0.0177	16
IEEE.802 (4,1)	1496	1	50 M - 15 G	Scattering	136	0.0127	26
INC	1286	196/54	10k - 9 G	Admittance	100	0.0189	271

Tab. 1. Implementation summary of different macromodeling examples.

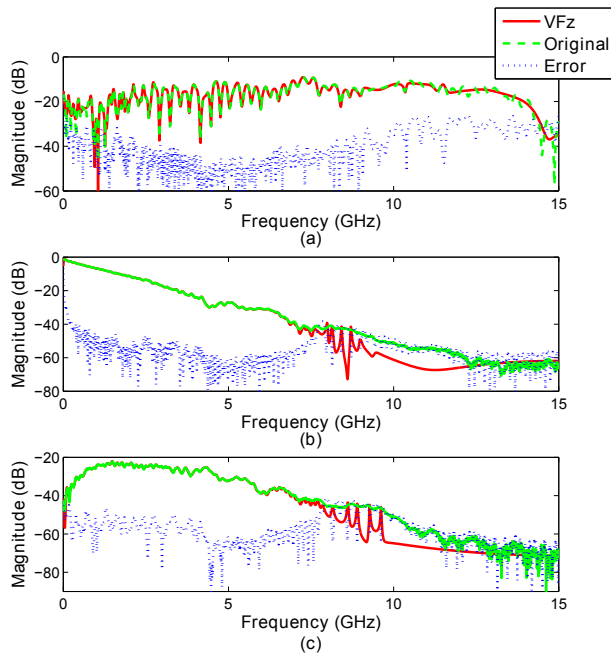


Fig. 3. Magnitude responses of the four-port backplane (4-port macromodeling: (a) Port (1,1), (b) Port (2,1) and (c) Port (4,1).

identification techniques and rational function macromodel. In some cases, interconnects are considered as electrically long for high-frequency circuits with time delay in the propagation of the signals. To handle this situation, delay extraction pre-processing is needed, or the response should be modeled using delay-based macromodels.

Fig. 3 shows the characteristics of the transmission channel. In Fig. 3(a) (Port (1,1)), we can observe a smaller (-20 dB) and then a larger return loss (-9 dB) in the lower- and higher-frequency reflection, respectively. An accurate identification is needed for the higher-frequency reflection because the upper envelopes characterize the overall worst-case reflection and the channel performance. In Fig. 3(b) (Port (2,1)), we can observe a visually smooth response with many small ripples, which is a typical measured insertion loss response. Fig. 3(c) (Port (4,1)) shows the crosstalk between channels, i.e., the coupling of signal from the aggressor to the victim. There is a -40 dB (1 %) coupling in the low frequency operation, and the coupling becomes -22 dB (8 %) when the frequency becomes 1.5 GHz. In high-speed digital

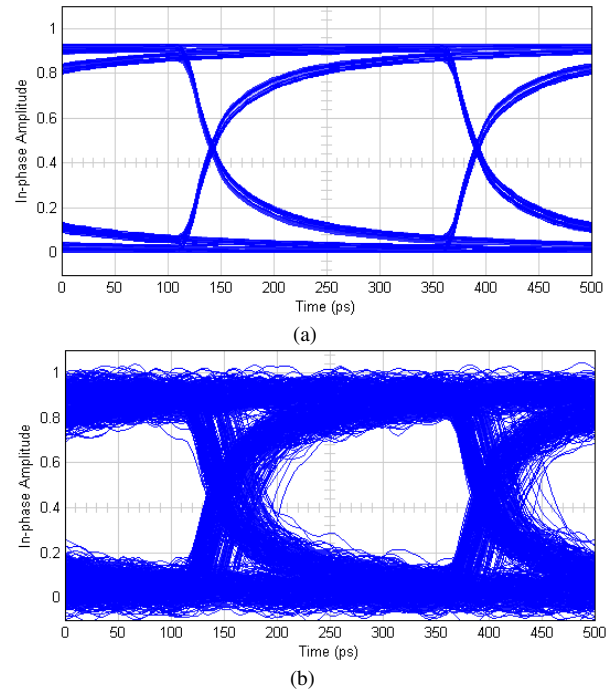


Fig. 4. Eye diagram of the channel: (a) uncorrupted input bit sequence, and (b) input bit sequence with Gaussian noise and Gaussian signal delay.

transmission, 1 % crosstalk can cause a significant deterioration and even a failure. Therefore, accurate channel identification and differential signaling are common practices in the high-speed electronic system design.

The obtained macromodel is used for a transient simulation on the Matlab-Simulink platform, as shown in Fig. 5. The model is excited by an uncorrupted 4000-bits random bit sequence (Bernoulli binary signal) with a pulse period of 5 ps (i.e., 20 Gbps bit rate). Also, the model is excited by the same configured bit sequence with noise (Gaussian distribution with zero mean and 0.03 variance) and signal delay (Gaussian distribution with zero mean and 15 variance). Eye diagrams are generated from the obtained signal. The eye diagram is updated simultaneously during the computation, and the final eye diagram is computed within 20 seconds. The eye diagram result in Fig. 5 shows that the digital signal is deteriorated during the transmission, and the corrupted signal can probably lead to an accidental signal mis-triggering. This means that SI analysis is necessary for modern high-speed circuit system design.

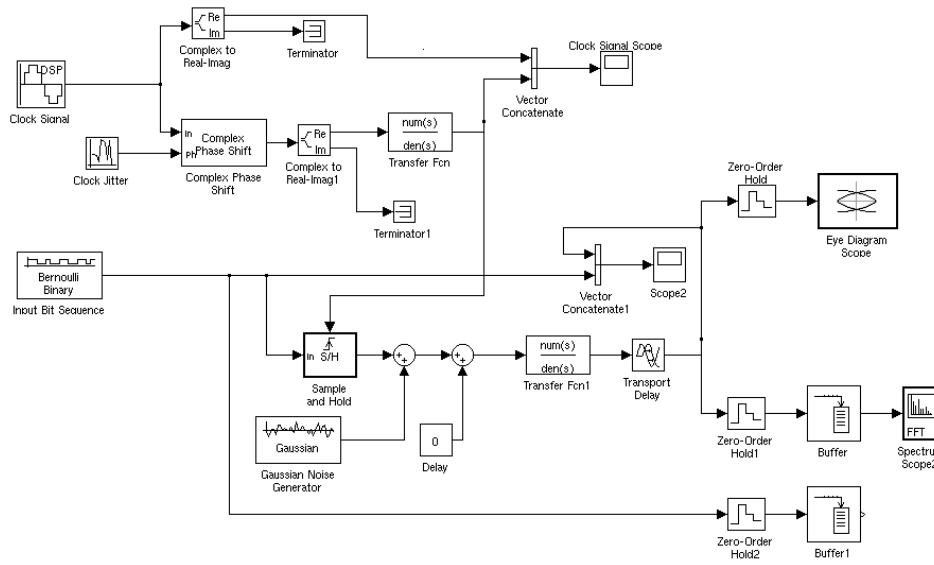


Fig. 5. Configuration of the backplane transient simulation in Matlab-Simulink, with clock jitter and transmission delay.

4.2 Macromodeling of the Crosstalk of a Four-port Backplane Using VFz

An Intel ATCA Ethernet backplane test system is designed, fabricated and measured for the IEEE 802.3 standardization. The backplane system contains line cards with via stubs, backplane, connectors and AC coupling capacitors. There are eight channels from three signaling layers in the backplane. The 4-port scattering parameters of the top signal signaling layers (IEEE.802) are measured at 1496 frequencies ranging from 50 MHz to 15 GHz. Frequency-sampled signals of some typical port responses are extracted. Each response is fitted using VFz with a 136-pole approximant. It takes about 12 iterations (16 seconds) and 20 iterations (26 seconds) for VFz to reach convergence of port response (3,1) and port response (4,1), respectively. Fig. 6 plots the fitted responses. The implementation analysis is summarized in Table 1. These promising results demonstrate the superiority of VFz in modeling board-level interconnect systems.

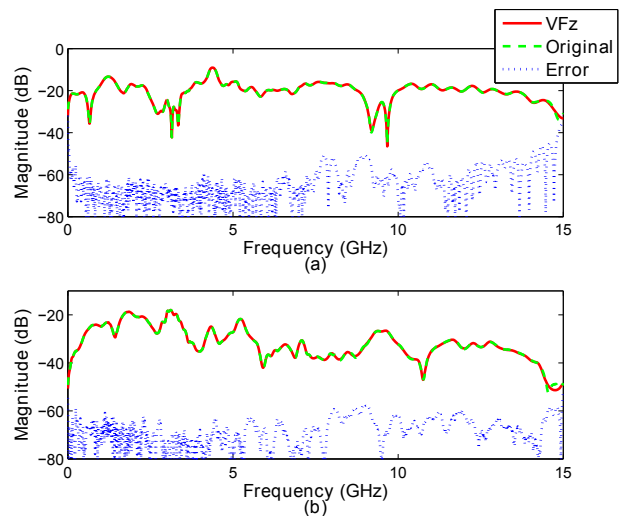


Fig. 6. Magnitude responses of the four-port Intel backplane (IEEE.802) macromodeling: (a) Port (3,1) and (b) Port (4,1).

4.3 Macromodeling of a Power Distribution Network of a System-In-Package Board Using VFz

The tested System-In-Package (SIP) intelligent network communicator (INC) board contains digital, radio frequency (RF) and optoelectronic sections on a single 83 mm × 65 mm test bed [15]. The board has two FPGA chips, one multiplexer (MUX), one RF amplifier, one signal layer, one irregularly shaped ground layer and one irregularly shaped power plane layer. A 14 × 14 admittance parameter matrix is generated. Fig. 7 plots the signal energy distribution of the approximated system, from which we can see that some pairs of ports are not coupled with each other. By extracting the coupled responses from all the responses, the approxi-

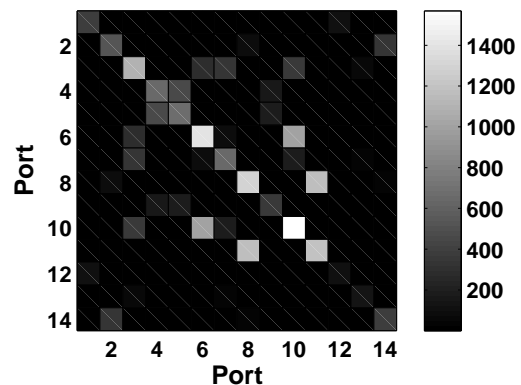


Fig. 7. Signal energy distribution of the power distribution network (INC) model.

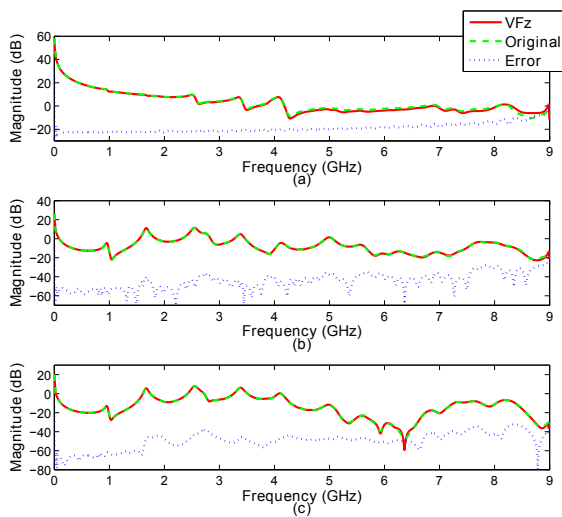


Fig. 8. Magnitude responses of the power distribution network (INC) macromodeling: (a) Port (6,10), (b) Port (7,13), and (c) Port (10,13).

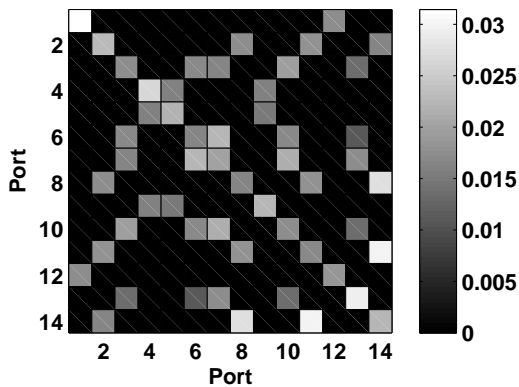


Fig. 9. Relative error energy distribution of the power distribution network (INC) macromodel.

mation is significantly reduced from fitting 196 responses to fitting 54 responses. The frequency-sampled responses are fitted using VFz with a 100-pole approximant. It takes 271 seconds and 5 iterations for VFz to converge, with the average relative error being 0.0189. The implementation analysis is summarized in Table 1. Fig. 8 plots approximation of some typical responses. Fig. 9 plots the distribution of the relative error of energy, and shows that the error distribution is independent to the energy distribution. This large-scale macromodeling example has a large amount of response data to be fitted, but VFz is computationally well-conditioned and gives an accurate approximation within a few iterations.

4.4 Modeling-Simulation Process of a Differential Channel using DCTT

The backplane example in Section 4.1 is used to show the efficiency and accuracy of DCTT. The example arises

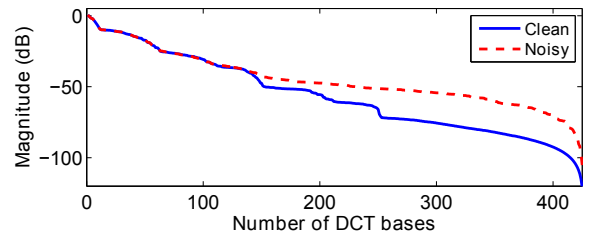


Fig. 10. Magnitude of the DCT bases of clean and noisy channels in the descending order.

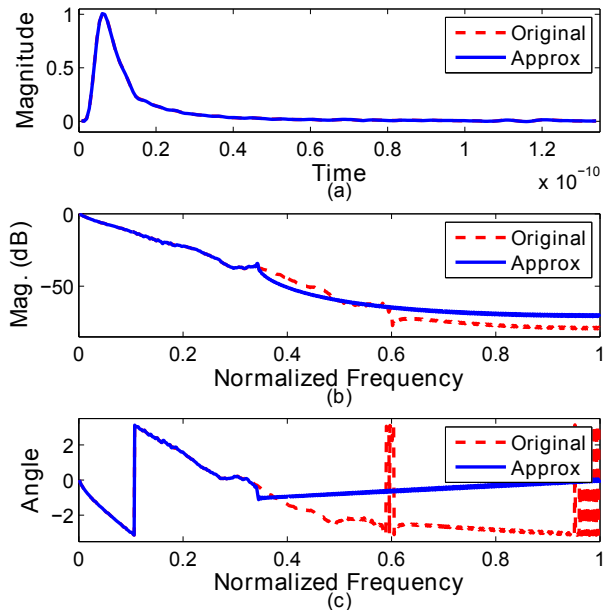


Fig. 11. (a) Time impulse responses, (b) magnitude responses and (c) phase responses of the clean differential channel example in the discrete-time frequency.

from modeling a differential transmission channel. The time-domain response is generated, normalized and fitted using DCTT. Time samples are taken at 0.67 ps intervals for the first 425 points (0.28 ns). The algorithm requires 0.023 seconds to decompose the signal into its DCT bases. As shown by the DCT basis energy distribution in Fig. 10, most energy is compacted by a small amount of DCT bases, therefore the least significant DCT bases can be truncated without loss of accuracy. DCTT requires 141 and 109 DCT bases to model the signal with a 1% and 3% relative error ($\|\text{error energy}\|_2 / \|\text{signal energy}\|_2$), respectively. Fig. 11 plots the normalized discrete-time frequency-domain responses and the normalized time-domain responses of the approximant with a 1% relative error, demonstrating the excellent fitting accuracy in both time and frequency (magnitude and phase) domains. Given a 2^{17} -points input signal sequences, DCTT requires 0.08 seconds to calculate the output response sequence, and the

transient response and the eye diagram of the channel are shown in Fig. 12. The system is also modeled using an eigenvalue-calculation-free algorithm (VISA [25]) using a 45th-order rational-function macromodel and 20 (converged) algorithm iterations. The quantitative data are shown in Tab. 2, which shows a significant ($\sim 9.94\times$) speed-up using DCTT due to its efficient single-step calculation.

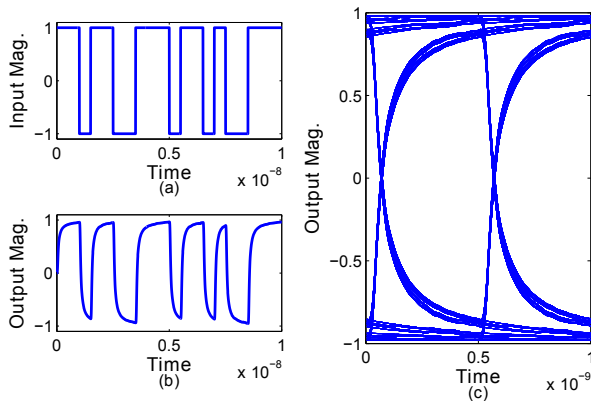


Fig. 12. (a) Time-domain random high-frequency input signal (the first 2000-points), (b) Output response of the differential channel using DCTT modeling (the first 2000 points) and (c) eye diagram of the modeled system using DCTT (2^{17} -points).

Next, we study the robustness of DCTT. First, we repeat the example with the response corrupted by white noise under a signal-to-noise ratio (SNR) of -30 dB ($\sim 3.14\%$ error). DCTT requires 116 DCT bases (7 additional DCT bases) to model the response with a 3% relative error. The magnitude of DCT bases are shown in Fig. 10. As shown in figure, the noise signals are decomposed and spread in the small-magnitude basis region, and most of them are truncated. Second, the differential channel example is repeated with different signal sequence lengths (longer impulse response tail). The quantitative result is shown in Tab. 3, which shows that there is a slight increase in computation time, and an increase of the required bases for longer sequences due to a wider spread of the DCT basis distribution.

	Channel			Crosstalk		Serial
	WISE	DCTT	DCTT (noisy)	WISE	DCTT	DCTT
Var #	45	141	118	55	251	664
Rel. err.	0.011	0.010	0.030	0.028	0.0298	0.030
Time (s)	0.348	0.035	0.036	0.417	0.062	0.077

Tab. 2. Comparison between DCTT and other algorithms in the examples.

Sequence length	200	425	600	800	1000
Number of var.	66	141	198	264	330
CPU Time (sec.)	0.031	0.035	0.039	0.042	0.046

Tab. 3. Comparison of DCTT in the differential channel example with different response sequence lengths.

4.5 Modeling-Simulation Process of a Crosstalk Response and a Serial-Link Type Response using DCTT

The example arises from modeling the bandpass-response crosstalk between transmission channels on the backplane in Section 4.1. The result is shown in Fig. 13 and Tab. 2. Fig. 13 shows that DCTT accurately approximates the response with a higher magnitude (region near $0.7f_s$, where f_s is the normalized sampling frequency).

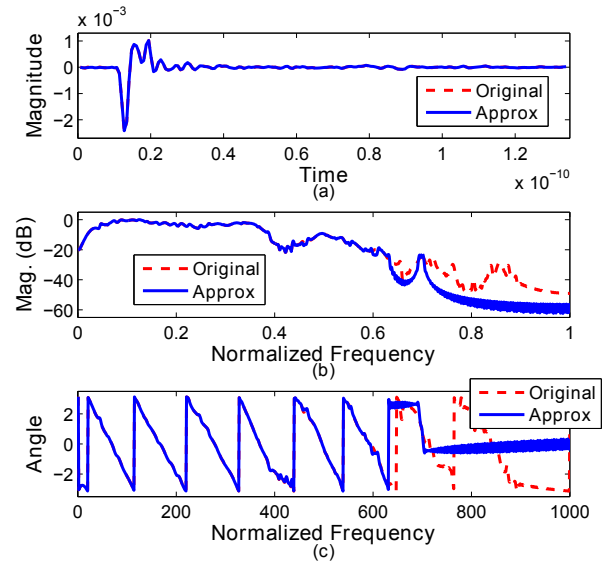


Fig. 13. (a) Time impulse responses, (b) magnitude responses and (c) phase responses of the crosstalk example in the discrete-time frequency.

Lastly, a complicated 2000-point impulse response of a serial-link type response is created and imported for macromodeling, which cannot be approximated effectively by iterative pole-finding calculation approaches. The modeling results are shown in Fig. 14 and Tab. 2, DCTT can accurately model complicated and long responses. In summary, it is a good choice to use non-iterative, numerically simple DCTT for the macromodeling process.

5. Conclusions

SIM-DSP framework has been presented for the macromodeling-simulation process. We have developed a digital signal processing (DSP) enhanced macromodeling-simulation process for signal integrity (SI) verifications. In particular, SIM-DSP framework, which is assembled by our core identification modules and peripheral modules, has improved the accuracy and functionality of the macromodeling process, through the validation from numerical examples. Furthermore, DCTT is also introduced for a single-step, numerical robust modeling-simulation of arbitrary port-to-port responses. Non-linear macromod-

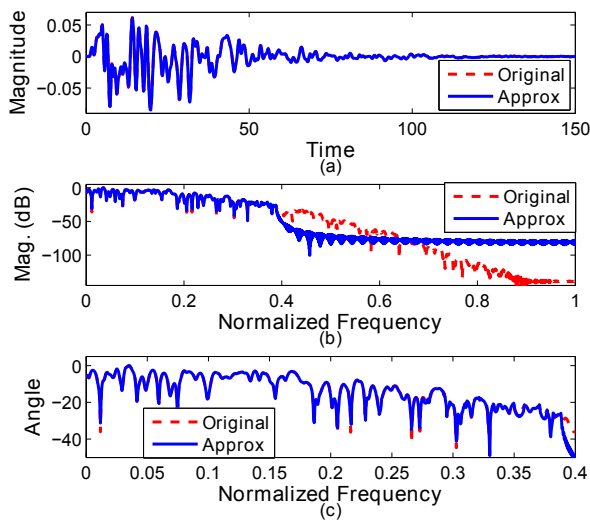


Fig. 14. (a) Time impulse responses, (b) magnitude responses and (c) low-frequency magnitude responses of the serial link-type example in the discrete-time frequency.

eling algorithms and multi-rate macromodeling-simulation process can be developed in the future to meet the simulation requirements of emerging circuit techniques.

References

- [1] DAVIS, J. A., VENKATESAN, R., KALOYEROS, A., et al. Interconnect limits on gigascale integration (GSI) in the 21st century. *Proceedings of the IEEE*, 2001, vol. 89, no. 3, p. 305 - 324.
- [2] GOUDOS, S. Calculation and modeling of EMI from integrated circuits inside high-speed network devices. *Radioengineering*, 2006, vol. 15, no. 4, p. 2 - 8.
- [3] LI, E.-P., WEI, X.-C., CANGELLARIS, A. C., LIU, E.-X., ZHANG, Y.-J., D'AMORE, M., KIM, J., SUDO, T. Progress review of electromagnetic compatibility analysis technologies for packages, printed circuit boards, and novel interconnects. *IEEE Transactions on Electromagnetic Compatibility*, 2010, vol. 52, no. 2, p. 248 - 265.
- [4] ARITRA, A., BANERJEE, S., BANERJEE, J. P. Large-signal simulation of 94 GHz pulsed silicon DDR IMPATTs including the temperature transient effect. *Radioengineering*, 2012, vol. 21, no. 4, p. 1218 - 1225.
- [5] HANY, F., CHEN, W., PISSOORT, D., BADESHA, A. Virtual-EMI lab: Removing mysteries from black-magic to a successful front-end design. In *Proceedings of IEEE Workshop on Signal Propagation on Interconnects*. Hildesheim (Germany), 2010, p. 105 - 108.
- [6] SANATHANAN, C., KOERNER, J. Transfer function synthesis as a ratio of two complex polynomials. *IEEE Transactions on Automatic Control*, 1963, vol. 8, no. 1, p. 56 - 58.
- [7] STEIGLITZ, K., MCBRIDE, L. E. A technique for the identification of linear systems. *IEEE Transactions on Automatic Control*, 1965, vol. 10, no. 4, p. 461 - 464.
- [8] GUSTAVSEN, B., SEMLYEN, A. Rational approximation of frequency domain responses by vector fitting. *IEEE Transactions on Power Delivery*, 1999, vol. 14, no. 3, p. 1052 - 1061.
- [9] CERNY, D., DOBES, J. Common lisp as simulation program (CLASP) of electronic circuits. *Radioengineering*, 2011, vol. 20, no. 4, p. 880 - 889.
- [10] *Official website of MATLAB RF toolbox*. [Online]. Available at: <http://www.mathworks.com/products/rftoolbox/>
- [11] *Official website of E-System Design*. [Online]. Available at: <http://www.e-systemdesign.com/>
- [12] ELFADEL, I. M., ANAND, M. B., DEUTSCH, A., et al. AQUAIA: A CAD tool for on-chip interconnect modeling, analysis, and optimization. In *Proceedings of IEEE Electrical Performance of Electronic Packaging Conference*. Monterey (CA, USA), 2002, p. 337 - 340.
- [13] ELFADEL, I. M., DEUTSCH, A., KOPCSAY, G. V., RUBIN, B. J., SMITH, H. H. A CAD methodology and tool for the characterization of wide on chip buses. *IEEE Transactions on Advanced Packaging*, 2005, vol. 28, no. 1, p. 63 - 70.
- [14] MIN, S. H., SWAMINATHAN, M. Construction of broadband passive macromodels from frequency data for simulation of distributed interconnect networks. *IEEE Transactions on Electromagnetic Compatibility*, 2004, vol. 46, no. 4, p. 544 - 558.
- [15] MIN, S. H. *Automated Construction of Macromodels from Frequency Data for Simulation of Distributed Interconnect Networks*, Ph.D. dissertation. Georgia Institute of Technology (USA), 2004.
- [16] NAREDO, L., RAMIREZ, A., AMETANI, A., et al. Z-transform-based methods for electromagnetic transient simulations. *IEEE Transactions on Power Delivery*, 2007, vol. 22, no. 3, p. 1799 - 1805.
- [17] BRENNER, P. A general modeling approach for linear circuit blocks and passive multiport components. In *Proceedings of IEEE European Packaging Workshop*, 2007.
- [18] DENK, G., FELDMANN, U. Circuit simulation for nanoelectronics. In *From Nano to Space*. Springer, 2008, p. 11 - 26.
- [19] LEI, C. U. *VLSI Macromodeling and Signal Integrity Analysis via Digital Signal Processing Techniques*, Ph.D. dissertation. Hong Kong: University of Hong Kong, 2011.
- [20] BOGATIN, E. *Signal and Power Integrity – Simplified*. Upper Saddle River (NJ, USA): Prentice Hall, 2010.
- [21] RESSO, M., BOGATIN, E. *Signal Integrity Characterization Techniques*. International Engineering Consortium, 2009.
- [22] YU, W. *Electromagnetic Simulation Techniques Based on the FDTD Method*. Wiley, 2009.
- [23] LEI, C. U. Exploiting implicit information from data for linear macromodeling. *IEEE Transactions on Components, Packaging and Manufacturing Technology*, 2013, vol. 3, no. 9, p. 1570 - 1577.
- [24] LEI, C. U., WONG, N. Efficient linear macromodeling via discrete-time time-domain vector fitting. In *Proceedings of International Conference on VLSI Design*. 2008, p. 469 - 474.
- [25] LEI, C. U., WONG, N. VISA: Versatile Impulse Structure Approximation for time-domain linear macromodeling. In *Proceedings of Asia and South Pacific Design Automation Conference*. Taipei (Taiwan), 2010, p. 37 - 42.
- [26] LEI, C. U., WONG, N. WISE: Warped Impulse Structure Estimation for time-domain linear macromodeling. *IEEE Transactions on Components, Packaging and Manufacturing Technology*, 2012, vol. 2, no. 1, p. 131 - 139.
- [27] BASEL, M., STEER, M., FRANZON, P. Simulation of high speed interconnects using a convolution-based hierarchical packaging simulator. *IEEE Transactions on Components, Packaging, and Manufacturing Technology, Part B: Advanced Packaging*, 1995, vol. 18, no. 1, p. 74 - 82.

- [28] ROY, S., DOUNAVIS, A. Transient simulation of distributed networks using delay extraction based numerical convolution. *IEEE Transactions on Components, Packaging, and Manufacturing Technology, Part B: Advanced Packaging*, 2011, vol. 30, no. 3, p. 364 - 373.
- [29] RAO, K. R., YIP, P. *Discrete cosine transform: algorithms, advantages, applications*. Academic Press Professional, 1990.
- [30] BODAPATI, S., NAJM, F. N. High-level current macro model for logic blocks. *IEEE Transactions on Computer-Aided Design of Integrated Circuits and Systems*, 2006, vol. 25, no. 5, p. 837 - 855.
- [31] AHMED, N., RAO, K. R. *Orthogonal Transforms for Digital Signal Processing*. Springer, 1975.
- [32] CHO, N. I., MITRA, S. K. Warped discrete cosine transform and its application in image compression. *IEEE Transactions on Circuits and Systems for Video Technology*, 2000, vol. 10, no. 8, p. 1364 - 1373.
- [33] GRIVET-TALOCIA, S., UBOLLI, A. A comparative study of passivity enforcement schemes for linear lumped macromodels. *IEEE Transactions on Advanced Packaging*, 2008, vol. 31, no. 4, p. 673 - 683.
- [34] SMITH, J. O. *Physical Audio Signal Processing for Virtual Musical Instruments and Audio Effects*. W3K Publishing, 2010.
- [35] VENKATARAMANI, B., BHASKAR, M. *Digital Signal Processors: Architecture, Programming and Applications*. Boston (MA, USA): McGraw-Hill Higher Education, 2002.
- [36] ZENG, R. X., SINSKY, J. H. Modified rational function modeling technique for high speed circuits. In *Proceedings of MTT-S International Microwave Symposium Digest*. 2006, p. 1951 - 1954.

About Authors...

Chi-Un LEI received his B.Eng. (first class honors) and Ph.D. in Electrical and Electronics Engineering from the University of Hong Kong in 2006 and 2011, respectively. He is now a Honorary Assistant Professor and a Research Scientist at the same university. His research interests include VLSI signal integrity analysis, cyber physical systems, learning analytics and engineering education.